

Detailed Analysis of Nearby Bulge-like Dwarf Stars I. Stellar Parameters, Kinematics and Oxygen Abundances

Luciana Pompéia and Beatriz Barbuy
Instituto Astronômico e Geofísico, USP, 01060-970 São Paulo, Brazil
 pompeia@iagusp.usp.br, barbuy@iagusp.usp.br
 and

Michel Grenon
Observatoire de Genève, Chemin des Maillettes 51, CH-1290 Sauverny, Switzerland
 Michel.Grenon@obs.unige.ch

ABSTRACT

High resolution échelle spectra were obtained with the FEROS spectrograph at the 1.5m ESO telescope for 35 nearby bulge-like stars with metallicities in the range $-0.8 \leq [\text{Fe}/\text{H}] \leq +0.4$. Geneva photometry, astrometric data from Hipparcos and radial velocities from Coravel are available for these stars. From Hipparcos data it appears that the turnoff of this population indicates an age of 10-11 Gyr (Grenon 1999).

Detailed analysis of the sample stars is carried out and atmospheric parameters derived from spectroscopic and photometric determinations are presented. Oxygen abundances are derived based on the forbidden [O I] λ 6300.3 Å line. The results show an oxygen overabundance pattern for most of the sample stars when compared to their disk counterparts.

Subject headings: stars: abundances - stars: chemical evolution - stars: late-type

1. Introduction

Stars in the solar neighborhood comprise a variety of stellar populations, with different kinematics, ages, chemical compositions and origins. The study of such populations can help understanding the formation and evolution of the Galaxy components.

With the aim of improving knowledge about these populations, an observational program of 7900 nearby stars was proposed for the Hipparcos mission, selected by M. Grenon, based on the NLTT proper motion catalogue (New Luyten Two Tenths Catalogue) (see Grenon 1999). Metallicities and temperatures were determined from Geneva photometry for 5500 of these stars.

Two subsamples of these stars, the MR (metal-rich) and the SMR (super metal-rich) stars, have been studied by Grenon (1972, 1989, 1990, 1999, 2000), where MR are defined as having metallicities $+0.08 \leq [\text{M}/\text{H}] \leq +0.20$ and the SMR have $[\text{M}/\text{H}] > +0.20$. Their isochronal ages revealed three groups with homogeneous ages: a group of the Hyades generation, with ~ 0.7 Gyr, an intermediate generation with 3-4 Gyr, and a very old component of \sim

10 Gyr.

The old SMR and MR population was found to be the flattest component of the solar neighborhood. The mean distance from the galactic plane for 219 of these SMR stars is only 0.16 kpc, which seems to be in contradiction with the classical σW vs. age relation.

The metallicity gradient of the galaxy indicates an inner disk or bulge origin for this component, in which case a mechanism of radial migration with very little scatter in scale heights is required. Mergers and stochastic shocks with molecular clouds were proposed but they trigger little angular momentum change in stellar motions (Grenon 2000 and references therein). The most efficient mechanism suggested is the action of a galactic bar in the inner disk and bulge structures. Models by Fux (1997) predict that the bar perturbation induces motions of most stars towards the galactic center. Many of these stars merge to the bulge population acquiring its dynamics. A tiny fraction gains radial energy and drifts to higher galactocentric radius. They form a thin disk which expands outwards with their initial σW nearly conserved (Grenon 1999, 2000, Raboud et al. 1998).

Sharing the same kinematical properties of the old MR and SMR samples, a collection of 612 NLTT nearby stars is found. This sample is restricted to objects with highly

¹Based on observations carried out at the European Southern Observatory, La Silla

eccentric orbits, pericentric distances $R_p < 5.5$ kpc, and absolute vertical velocities of less than 20 km s^{-1} . The metallicity distribution of this flat component is identical to that seen in the bulge by McWilliam & Rich (1994). Solar ratios are expected for disk stars while $[\alpha/\text{Fe}] \geq 0$ values are expected for bulge stars due to a fast chemical enrichment at early times, and a consequent dominant contribution by Type II SNe (Matteucci & Brocato 1990, Matteucci et al. 1999, Mollá et al. 2000).

In the present work a subsample of the bulge-like stars with metallicities in the range $-0.8 \leq [\text{Fe}/\text{H}] \leq +0.4$ is studied. Detailed analyses are carried out and oxygen abundances are derived. In Sect. 2 the kinematical properties of the sample are reported. In Sect. 3 the observations and reductions are described. In Sect. 4 the effective temperatures, gravities and metallicities are derived. Oxygen abundances are presented in Sect. 5. The results are discussed in Sect. 6 and in Sect. 7 a summary is given.

2. Kinematics, Observations and Reductions

The present sample consists of stars with very eccentric orbits ($e > 0.25$), maximum distances to the galactic plane $Z_{\text{max}} < 1$ kpc, and pericentric distances R_p , as small as 2-3 kpc. Their V space velocities are between -50 to -130 km s^{-1} while the U velocities are from -150 to $+100 \text{ km s}^{-1}$. Basic kinematical properties are reported in Table 1. Proper motions are from the NLTT catalog and the orbital parameters R_p and R_a were deduced using a galactic potential model by Magnenat (1982 and private communication, 1984), assuming the following solar parameters: galatocentric distance $R_\odot = 8.0$ kpc, circular velocity $V_c = 228.7 \text{ km s}^{-1}$ and local density of $0.15 M_\odot/\text{pc}^3$ (Grenon 1987a, 1987b). Heliocentric radial velocities were determined from a list of Ca I, Na I, Fe I and Mg I lines in the spectral range 6000 - 7600 Å.

The observations were carried out at the 1.52m telescope at ESO, La Silla, using the Fiber Fed Extended Range Optical Spectrograph (FEROS) (Kaufer et al. 2000). The total spectrum coverage is 356 nm - 920 nm, with a resolving power of 48,000. Two fibers, with entrance aperture of 2.7 arcsec, recorded simultaneously star light and sky background. The detector is a back-illuminated CCD with 2048×4096 pixels of $15 \mu\text{m}$ size.

Sample stars were observed on five nights, September 22-26, 1999. Using a special package for reductions (DRS) of FEROS data, in MIDAS environment, the data reduction proceeded with subtraction of bias and scattered light in the CCD, orders extraction, flat fielding, and wavelength calibration with a ThAr calibration frame.

Table 2 gives basic data for the sample stars: a short designation given in the present work, identification, V magnitude from Hipparcos, spectral type, distance (pc), reddening $E(\text{B}-\text{V})$, M_v (dereddened values),

bolometric correction BC, stellar mass (M_*/M_\odot), and the signal to noise ratio S/N. The S/N ratio was calculated and averaged for five regions free from lines. The reddening was derived by using the code Extinct from Hakkila et al. (1997) and using the option of extinction by Arenou et al. (1992). Bolometric corrections were inferred from the theoretical calibrations of Lejeune, Cuisinier & Buser (1997). Stellar masses were derived from isochrones of Vandenberg (1985) and Vandenberg & Laskarides (1987).

3. Atmospheric Parameters

3.1. Temperatures

3.1.1. Photometry

Geneva photometry was used to estimate the effective temperatures T^{Gen} , by applying the calibration given in Grenon (1982). The derived values are given in Table 3.

The effective temperatures were also calculated from Stromgren colors given in Hauck & Mermilliod (1998). The Stromgren colors were transformed to temperatures T^{Strom} according to relation (9) given in Alonso et al. (1999). Stromgren colors were then dereddened assuming the relation of $E(\text{b}-\text{y}) = 0.13 E(\text{B}-\text{V})$ given in Crawford & Mandwewala (1976).

Alonso et al. (1996) and Blackwell et al. (1990) used the InfraRed Flux Method (IRFM) to derive the temperatures of a sample of F0-K5 dwarfs, among which 3 stars of the present sample. In Table 3 are reported the resulting temperatures T^{Gen} , T^{Strom} and T^{IRFM} for the sample stars.

3.1.2. $H\alpha$ profiles

Spectroscopic temperatures were derived using $H\alpha$ profiles. These profiles were computed with MARCS model atmospheres (Gustafsson et al. 1975) and a revised version of the code HYDRO by Praderie (1967). The temperatures which better reproduce the $H\alpha$ wings profiles were chosen. The continuum level was set using continuum regions on the red and blue sides of the Balmer feature. The reliability of temperatures derived from hydrogen lines profiles was discussed by Fuhrmann et al. (1993, 1994), by comparing temperatures determined from Balmer lines with those from photometric data. They found a smaller scatter among temperatures derived from Balmer lines than among those derived from the photometric indices $b - y$ and $V - K$.

In Fig. 1 we show the fit of the computed $H\alpha$ wings to the observed profile of HD 179764. Synthetic spectra were computed for $T_{\text{eff}} = 5350 \text{ K}$, 5450 K and 5450 K . In Table 3 $T^{\text{H}\alpha}$ values are given.

The mean differences of $T^{\text{H}\alpha}$ relative to T^{Gen} and T^{Strom} are $\Delta(T^{\text{H}\alpha} - T^{\text{Gen}}) = 49 \text{ K}$ with a standard deviation $\sigma = 42 \text{ K}$, and $\Delta(T^{\text{H}\alpha} - T^{\text{Strom}}) = 69 \text{ K}$ with σ

= 54 K. Note that Fuhrmann et al. (1994) calculated the temperature of HD 143016 using $H\beta$ profiles computed with models scaled to empirical solar models. They found $T_{\text{eff}} = 5650$ K for this star, in good agreement with our derived value of $T_{\text{eff}} = 5575$ K.

Model atmospheres were checked for ten of our stars using two other grids of models, OSMARCS by Edvardsson et al. (1993) and ATLAS by Kurucz (1993). We also calculated temperatures with $H\beta$ profiles $T^{H\beta}$, using MARCS models. The resulting T^{Kur} for Kurucz (1993) models, T^{Edv} for Edvardsson et al. (1993) models, and $T^{H\beta}$ are shown in Table 4 (the spectrum of CD-40 15036 has a bump in the $H\beta$ region, and $T^{H\beta}$ was not derived for this star). There is good agreement among the different temperature indicators and we adopted $T^{H\alpha}$ as final temperature values.

3.2. Gravities

Trigonometric gravities were derived using Hipparcos parallaxes through the classical formula:

$$\log g/g_{\odot} = \frac{M_*}{M_{\odot}} + 4\log \frac{T_*}{T_{\odot}} + 0.4V + 0.4BC + 2\log \pi + 0.12$$

Spectroscopic gravities were calculated by requiring that Fe I and Fe II yield the same iron abundance. The line lists were selected from Castro et al. (1997), Nave et al. (1994) and from the NIST Atomic Spectra Database (physics.nist.gov/cgi-bin/AtData/main-asd). Using the Atlas of the Solar Photosphere (Wallace, Hinkle and Livingston 1998) a check of possible blends was performed and blended lines were discarded. The line lists of Fe I and Fe II are given in Tables 5 and 6 respectively. The log gf values are from NIST and the adopted solar abundances are from Grevesse et al. (1996).

The results for log g from Hipparcos parallaxes and ionization equilibrium are given in Table 11. The average difference between the two methods is of 0.15 dex. Discrepancies between these methods have been pointed out by Edvardsson (1988), Nissen et al. (1997), Fuhrmann et al. (1997) and Allende Prieto et al. (1999, hereafter AGLG99) in the sense that trigonometric gravities are higher than spectroscopic ones. AGLG99 studied the trigonometric and spectroscopic gravities available in the literature, revealing that the absolute differences are small for stars in the metallicity range $-1.0 < [\text{Fe}/\text{H}] < 0.3$, with a mean < 0.10 dex. For the present sample a mean difference $\Delta(\log g^{\text{Spec}} - \log g^{\text{Hip}}) = 0.19$ dex is found with a standard deviation $\sigma = 0.14$, in agreement with the AGLG99 results. We have adopted the spectroscopic gravities hereafter.

3.3. Metallicities and Microturbulent Velocities

The metallicities $[\text{Fe}/\text{H}]$ and microturbulent velocities ξ_t were derived using curves of growth of Fe I and Fe II.

The curves were built with the code RENOIR by M. Spite. Equivalent widths were measured using IRAF. The S/N of the spectra is high (Table 2) and the continua are well-defined.

Curves of growth for Fe I and Fe II of HD 179764 are given in Fig. 2. Equivalent widths of Fe I are given in Tables 7 and 8 and those of Fe II in Tables 9 and 10. Figs. 2a, b show the curves of growth of Fe I and Fe II for HD 179764. Metallicities inferred from Geneva photometry are also shown. In Table 11 the resulting values of $[\text{Fe}/\text{H}]$ and ξ_t are reported.

Small differences are found between photometric and spectroscopic metallicities: the mean value of the difference is 0.16 dex with a standard deviation of 0.15 dex. The final adopted values $[\text{Fe}/\text{H}]^{\text{Spec}}$ are given in Table 11.

4. Oxygen Abundances

Oxygen abundances were derived by comparing the observed $[\text{O I}]$ 6300.3 Å line to synthetic spectra. The log gf value was adopted from Castro et al. (1997). The spectrum synthesis code is described in Barbuy (1988) and Barbuy & Erdelyi-Mendes (1989). This line is insensitive to NLTE effects (Kiselman 2001). Telluric lines are removed by subtracting the spectrum of hot and rapidly rotating stars. In Figs. 3a,b we show the fit of the $[\text{O I}]$ line for HD 149256 and HD 148530. In Table 12 the resulting oxygen abundances are given. Spectrum synthesis analysis to infer other α and heavy elements abundances is in progress and will be presented elsewhere.

4.1. Abundance Errors

The abundances derived from the $[\text{O I}]$ line are not very sensitive to temperature. A variation of $\Delta T_{\text{eff}} = 100$ K induces $\Delta[\text{O}/\text{Fe}] \approx 0.05$ dex. Oxygen abundances are also almost insensitive to microturbulent velocity and $[\text{Fe}/\text{H}]$ uncertainties, $\Delta\xi_t = 0.2$ kms $^{-1}$ and $\Delta[\text{Fe}/\text{H}] = 0.2$ dex will result in $\Delta[\text{O}/\text{Fe}] \approx 0.05$ and 0.02 respectively. $[\text{O}/\text{Fe}]$ values are somewhat more sensitive to the gravity choice: $\Delta\log g = 0.2$ gives $\Delta[\text{O}/\text{Fe}] = 0.1$, but the errors in gravities are smaller than 0.2 dex, as shown by the differences between spectroscopic and trigonometric values.

In order to test how changes in atmospheric parameters correlate with each other and with the derived oxygen abundance we have applied changes in the temperature of a few stars to values ± 100 K the inferred one. For the lower temperatures, the ionization balance gives average gravity and metallicity values 0.2 dex and 0.06 dex below the derived ones, respectively, and the resulting $[\text{O}/\text{Fe}]$ ratio changes by 0.06 dex. For the higher temperatures, the ionization balance gives average gravity and metallicity values 0.15 dex above and 0.07 dex below the derived ones, respectively, and the resulting $[\text{O}/\text{Fe}]$ ratio

changes by 0.12 dex.

5. Discussion

In Fig. 4 the [O/Fe] ratio is plotted against [Fe/H] for the present sample, including also SMR stars studied by Barbuy & Grenon (1990) and a sample of disk stars by Nissen & Edvardsson (1992). The oxygen abundances of both samples were determined from the [O I] 6300 Å line. Theoretical curves of inside-out models by Matteucci et al. (1999) for the bulge (solid line), and by Chiappini et al. (2001) for the solar neighborhood (dotted line), are also plotted.

We found a higher [O/Fe] ratio for most of our stars when compared to their disk counterparts, although some of them show a disk-like pattern. Barbuy & Grenon (1990) also found an enhanced oxygen abundance for a SMR sample. A possible interpretation to such overabundance is that the flat component stars originate in a region of the Galaxy where the chemical evolution occurred faster than in solar neighborhood.

It is also apparent from Fig. 4 that the [O/Fe] ratios are below the predicted theoretical bulge curve. In this model (Matteucci et al. 1999) a fast collapse of 10^8 yr is assumed. Nevertheless, Maciel (2001), based on oxygen abundances of bulge planetary nebulae, suggested that the theoretical [O/Fe] vs. [Fe/H] curve from Matteucci et al. (1999) overestimates the [O/Fe] ratio by 0.3 to 0.5 dex, claiming that the discrepancy between the bulge theoretical curve and the solar neighborhood curve is smaller.

6. Summary

High resolution spectra of stars with $-0.8 \leq [\text{Fe}/\text{H}] \leq +0.4$ and isochronal ages of ~ 10 Gyr were obtained with the FEROS spectrograph. The sample stars have kinematical properties typical of a bulge or inner disk origin.

The main results from the present work are:

(1) Temperatures derived from photometric data (Geneva and Stromgren), IRFM, and H α profiles show small discrepancies (< 100 K) for most of the stars, with mean differences of ~ 70 K.

(2) A good agreement between spectroscopic (ionization equilibrium) and trigonometric gravities is also found, with a mean difference of 0.19 dex.

(3) A mean difference of 0.16 dex is found for the derived metallicities from Geneva photometry and from curves of growth of Fe I and Fe II.

(4) The curves for [O/Fe] vs. [Fe/H] show that most of our sample stars are overabundant in oxygen with respect to disk stars with the same metallicity.

Acknowledgments

L.P. thanks J. Melendez for very useful discussions.

We thank C. Chiappini, F. Matteucci and D. Romano for sending the theoretical curves of oxygen chemical enrichment. L. P. acknowledges the FAPESP PhD fellowship n $^\circ$ 98/00014-0. We acknowledge FAPESP project n $^\circ$ 1998/10138-8.

REFERENCES

- Alonso, A., Arribas, S., Martínez-Roger, C. 1996 A&AS, 117, 227
- Alonso, A., Arribas, S., Martínez-Roger, C. 1999, A&AS, 140, 261
- Allende Prieto, C., García López, R., Lambert, D.L., Gustafsson, B. 1999, ApJ, 527, 879
- Arenou, F., Grenon, M., Gomez, A. 1992, A&A 258, 104
- Barbuy, B. 1988, A&A, 191, 121
- Barbuy, B., Erdelyi-Mendes, M. 1989, A&A, 214, 239
- Barbuy, B. & Grenon, M., 1990. In Bulges of Galaxies, 1st ESO / CTIO workshop, ESO Workshop and Conference Proceedings no 35, eds B. Jarvis, D. Terndrup, (ESO: Garching bei München), 83
- Blackwell, D. E., Petford, A. D., Arribas, S., Haddock, D. J., Selby, M. J. 1990, A&A, 232, 396
- Castro, S., M. Rich, R., Grenon, M., Barbuy, B., McCarthy, J. 1997, ApJ 114, 1
- Chiappini, C., Matteucci, F., Romano, D. 2001, astro-ph/0102134
- Crawford, D. L., Mandwewala, N. 1976, PASP, 88, 917
- Edvardsson, B. 1988, A&A, 190, 148
- Edvardsson, B. Andersen, J., Gustafsson, B., Lambert, D. L., Nissen, P. E., Tomkin, J. 1993, A&A, 275, 101
- Fuhrmann, K., Axer, M., Gehren, T. 1993, A&A, 271, 451
- Fuhrmann, K., Axer, M., Gehren, T. 1994, A&A, 285, 585
- Fuhrmann, K., Pfeiffer, M., Frank, C., Reetz, J., Gehren, T. 1997, A&A, 323, 909
- Fux, R. 1997, A&A, 327, 983
- Grenon, M. 1972. Age des Etoiles, Proceedings of IAU Colloq. 17, held in Paris, France, G. Cayrel de Strobel and A. M. Delplace (eds.). Observatoire de Paris-Meudon, p.55
- Grenon, M. 1982, IAU Col. 68, 393
- Grenon, M. 1987a, J. Ap. & Astr. 8, 123
- Grenon, M. 1987b, in ESO Conf. and Workshop: Stellar Evolution and Dynamics in the Outer Halo of the Galaxy, eds. M. Azzopardi and F. Matteucci, Garching, p. 123
- Grenon, M. 1989, Ap&SS, 156, 29
- Grenon, M. 1990, in Bulges of Galaxies, 1st ESO / CTIO workshop, ESO Workshop and Conference Proceedings n. 35, eds B. Jarvis, D. Terndrup, (ESO: Garching bei München), 143
- Grenon, M. 1998, in Highlights of Astronomy, ed. J. Andersen, vol.11A, p. 560
- Grenon, M. 1999, Ap&SS, 265, 331

- Grenon, M. 2000, in *The Evolution of the Milky Way*, F. Matteucci and F. Giovannelli (eds.), Kluwer Academic Publishers, 47
- Grevesse, N., Noels, A., Sauval, J. 1996, in *ASP Conf. Ser.* 99, eds. S.S. Holt, G. Sonneborn, p. 117
- Gustafsson, B., Bell, R. A., Eriksson, K., Nordlund, A. 1975, *A&A*, 42, 407
- Hauck, B., Mermilliod, M. 1998, *A&AS*, 129, 431
- Hakkila, Jon, Myers, Jeannette M., Stidham, Brett J., Hartmann, Dieter H. 1997, *AJ* 114, 2043
- Kaufer, A., Stahl, O., Tubbesing, S., Norregaard, P., Avila, G., Francois, Pasquini, L., Pissella, A. 2000, in *Proc. SPIE* Vol. 4008, 459
- Kiselman, D. 2001, *NARv.*, 45, 559
- Kurucz, R. 1993, *ATLAS9 Stellar Atmosphere Programs and 2 kms⁻¹ grid*. Kurucz CD-ROM No. 13. Cambridge, Mass., Smithsonian Astrophysical Observatory
- Lejeune, Th., Cuisinier, F., Buser, R. 1997, *A&AS*, 125, 229
- Maciel W.J., 2001, *NARv.*, 45, 571
- Matteucci, F., Brocato, E. 1990, *ApJ*, 365, 539
- Matteucci, F., Romano, D., Molaro, P. 1999, *A&A*, 341, 458
- Magenat, P. 1982, *Cel. Mech.* 28, 319
- Magenat, P. 1984, private communication
- McWilliam, A., Rich, R. M. 1994, *ApJS*, 91, 749
- Mollá, M., Ferrini, F., Gozzi, G. 2000, *MNRAS* 316, 345
- Nave, G., Johansson, S., Learner, R. C. M., Thorne, A. P., Brault, J. W. 1994, *ApJS* 94, 221
- Nissen, P. E., Edvardsson, B. 1992, *A&A*, 261, 255
- Nissen, P. E., Hoeg, E., Schuster, W. J., 1997, *ESASP* 402, 225
- Praderie, F. 1967, *Ann. Ap.*, 30, 31
- Raboud D., Grenon M., Martinet L., Fux L., Udry S. 1998, *A&A*, 335, L67
- Vandenberg, D. A. 1985, *ApJS*, 58, 561
- Vandenberg, D. A., Laskarides, P. G. 1987, *ApJS*, 64, 103
- Wallace, L., Hinkle, K., Livingston, W. 1998, in *An Atlas of the Solar Photosphere, from 13.500 to 28.000 cm⁻¹*, N. S. O. Technical report #98-001, National Solar Observatory, National Optical Astronomy Observatory

TABLE 1
KINEMATICAL DATA

Name	U	V	W	V_{Helio}	Rp	Ra
HD 143016	-3.2	-88.6	26.3	9.16(0.18)	3.80	8.02
HD 143102	52.9	-92.5	-19.6	7.44(0.11)	3.58	8.23
HD 148530	-80.8	-79.9	-34.1	25.27(0.14)	3.83	9.15
HD 149256	-7.0	-98.4	-48.1	25.10(0.07)	3.40	8.04
HD 152391	-85.2	-110.1	8.8	45.19(0.24)	2.78	9.01
HDE 326583	-45.0	-100.4	-39.4	74.42(0.27)	3.25	8.36
HD 175617	-121.3	-72.9	-28.7	71.00(0.17)	3.79	10.56
HD 178737	-8.3	-92.4	64.7	34.59(0.17)	3.64	8.04
HD 179764	21.2	-106.3	6.1	-66.40(0.16)	3.11	8.01
HD 181234	5.3	-91.7	1.8	-46.77(0.13)	3.68	8.00
HD 184846	-5.1	-123.7	-42.6	91.22(0.13)	2.48	8.02
BD-176035	35.0	-82.9	10.6	-65.85(0.12)	4.02	8.09
HD 198245	4.4	-128.2	21.6	-20.63(0.30)	2.34	8.00
HD 201237	-85.9	-79.0	-0.8	30.17(0.05)	3.83	9.29
HD 211276	-20.7	-105.9	-36.6	-24.30(0.17)	3.10	8.11
HD 211532	73.1	-87.4	49.9	-111.24(0.20)	3.70	8.52
HD 211706	80.1	-106.1	-12.6	-63.11(0.17)	2.99	8.55
HD 214059	99.1	-101.6	-112.8	-11.77(0.12)	3.08	8.93
C-40 15036	88.4	-79.7	-9.1	-13.04(0.15)	3.91	8.86
HD 219180	59.6	-89.9	2.0	-29.41(0.20)	3.66	8.32
HD 220536	7.4	-96.7	2.1	1.34(0.21)	3.48	8.00
HD 220993	-22.4	-96.7	-18.9	51.30(0.18)	3.44	8.13
HD 224383	74.5	-84.4	-0.8	-31.01(0.26)	3.81	8.56
HD 4308	-51.5	-110.4	-29.5	95.69(0.16)	2.87	8.41
HD 6734	-51.2	-122.6	38.1	-94.49(0.15)	2.47	8.38
HD 8638	26.1	-86.3	-77.7	84.67(0.27)	3.89	8.04
HD 9424	57.0	-96.5	-1.5	43.34(0.19)	3.41	8.27
HD 10576	55.9	-92.6	-19.2	54.39(0.19)	3.57	8.27
HD 10785	34.3	-103.1	13.7	-5.13(0.15)	3.21	8.07
HD 11306	26.7	-97.3	-19.1	64.88(0.22)	3.45	8.03
HD 11397	-19.1	-93.3	-49.7	41.05(0.15)	3.58	8.11
HD 14282	74.6	-90.4	41.3	0.19(0.26)	3.58	8.53
HD 16623	-12.4	-91.2	2.8	17.87(0.32)	3.68	8.07
BD-02 603	-46.8	-112.4	-48.2	6.55(0.19)	2.81	8.35
HD 21543	57.6	-91.5	-19.9	64.22(0.24)	3.60	8.29

TABLE 2
SAMPLE STARS.

Number	Name	V	Spectral Type	r(pc)	E(B-V)	M_V	BC	M_*/M_\odot	S/N
b1	HD 143016	8.50	G3V	58.11	0.094	4.40	-0.274	0.85 ¹	154
b2	HD 143102	7.88	G6IV/V	70.77	0.027	3.55	-0.231	1.10 ¹	127
b3	HD 148530	8.81	G9V	46.51	0.040	5.35	-0.307	0.90 ¹	120
b4	HD 149256	8.42	G8IV	75.07	0.077	3.80	-0.311	0.80 ²	71
b5	HD 152391	6.65	G8V	16.94	0.033	5.40	-0.299	0.90 ¹	133
b6	HDE326583	9.48	G0	143.88	0.101	3.38	-0.222	1.00 ¹	121
b7	HD 175617	10.12	G5	74.74	0.100	5.44	-0.265	0.80 ¹	124
b8	HD 178737	8.72	G2/G3V	86.28	0.049	3.89	-0.274	0.90 ¹	125
b9	HD 179764	9.01	G5	62.58	0.056	4.85	-0.250	0.90 ²	129
b10	HD 181234	8.59	G5	48.80	0.045	5.01	-0.311	0.90 ²	91
b11	HD 184846	8.95	G5V	81.83	0.037	4.27	-0.262	0.85 ¹	118
b12	BD-176035	10.30	-	70.27	0.037	5.95	-0.538	0.85 ²	54
b13	HD 198245	8.94	G3V	59.59	0.033	4.96	-0.274	0.80 ¹	151
b14	HD 201237	10.10	K2III	89.05	0.045	5.21	-0.538	0.95 ²	73
b15	HD 211276	8.72	G5	66.49	0.034	4.50	-0.372	0.85 ¹	195
b16	HD 211532	9.31	G5	52.74	0.015	5.65	-0.316	0.80 ¹	160
b17	HD 211706	8.90	G0	84.89	0.041	4.13	-0.206	1.00 ¹	136
b18	HD 214059	8.26	G4V	80.45	0.021	3.67	-0.265	0.90 ¹	142
b19	CD-4015036	10.08	G5V	93.02	0.033	5.14	-0.312	0.90 ¹	107
b20	HD 219180	9.81	G5V	80.39	0.032	5.18	-0.274	0.80 ¹	132
b21	HD 220536	9.01	G1V	87.72	0.032	4.19	-0.217	0.95 ¹	112
b22	HD 220993	9.34	G3V	92.59	0.032	4.41	-0.262	0.90 ¹	118
b23	HD 224383	7.89	G2V	47.66	0.032	4.40	-0.206	1.00 ¹	126
b24	HD 4308	6.55	G5V	21.85	0.011	4.82	-0.265	0.90 ¹	149
b25	HD 6734	6.44	K0IV	46.45	0.032	3.01	-0.363	1.05 ¹	163
b26	HD 8638	8.29	G3V	40.40	0.032	5.16	-0.265	0.85 ¹	153
b27	HD 9424	9.17	G8V	59.03	0.049	5.16	-0.312	0.90 ¹	104
b28	HD 10576	8.51	G0/G1V	85.76	0.062	3.65	-0.201	1.00 ¹	145
b29	HD 10785	8.51	G1/G2V	70.03	0.032	4.19	-0.211	0.95 ¹	159
b30	HD 11306	9.24	G8V	75.02	0.057	4.69	-0.321	0.85 ¹	144
b31	HD 11397	8.96	G6IV/V	54.64	0.032	5.17	-0.282	0.80 ¹	147
b32	HD 14282	8.39	G0	87.72	0.032	3.58	-0.226	0.95 ¹	127
b33	HD 16623	8.76	G2V/VI	65.88	0.032	4.57	-0.235	0.90 ¹	108
b34	BD-02 603	9.03	G0	109.53	0.044	3.70	-0.253	0.90 ¹	97
b35	HD 21543	8.23	G2V/VI	45.50	0.020	4.88	-0.249	0.70 ¹	135

REFERENCES.—(1) Vandenberg (1985), (2) Vandenberg & Laskarides (1987)

TABLE 3
EFFECTIVE TEMPERATURES

Number	T ^{Gen}	T ^{Hα}	T ^{Strom}	T ^{IRFM}	Number	T ^{Gen}	T ^{Hα}	T ^{Strom}	T ^{IRFM}
b1	5575	5575	-	-	b19	5340	5350	-	-
b2	5432	5500	5397	-	b20	5417	5400	-	-
b3	5346	5350	5576	-	b21	5829	5850	5868	-
b4	5271	5350	-	-	b22	5599	5600	-	-
b5	5335	5300	5366	-	b23	5689	5800	5715	-
b6	5629	5600	-	-	b24	5581	5600	5609	-
b7	5456	5550	5451	5656 ¹	b25	5021	5000	5000	-
b8	5495	5575	-	-	b26	5469	5500	5445	-
b9	5373	5450	-	-	b27	5332	5350	5358	-
b10	5220	5350	5201	-	b28	5883	5850	5915	-
b11	5587	5600	5593	-	b29	5773	5850	5782	-
b12	4830	4750	-	-	b30	5207	5200	5253	-
b13	5588	5650	5606	-	b31	5435	5400	5412	-
b14	4886	4950	-	-	b32	5790	5800	-	-
b15	5372	5500	5404	-	b33	5714	5700	5851	-
b16	5295	5350	-	-	b34	5476	5450	-	-
b17	5830	5800	5865	-	b35	5625	5650	5613	5568 ¹
b18	5468	5550	5504	5553 ²					

REFERENCES.—(1) Alonso et al. (1996), (2) Blackwell et al. (1990)

TABLE 4
EFFECTIVE TEMPERATURES CHECK

Number	T ^{Gen}	T ^{Hα}	T ^{Edv}	T ^{Kur}	T ^{Hβ}	T ^{Strom}
b01	5575	5575	5575	5500	5575	-
b14	4886	4950	4750	4750	4950	-
b15	5372	5500	5400	5500	5500	5404
b19	5340	5350	5250	5250	-	-
b22	5599	5600	5500	5500	5600	-
b23	5689	5800	5700	5750	5800	5715
b25	5021	5000	5000	5000	5000	5000
b28	5883	5850	5850	5750	5850	5915
b29	5773	5850	5750	5750	5850	5782
b30	5207	5200	5200	5000	5200	5253

TABLE 5
FE I LINE LIST.

Ion	$\lambda(\text{\AA})$	χ_{ex}	log gf	Ion	$\lambda(\text{\AA})$	χ_{ex}	log gf
Fe I	6056.005	4.73	-0.46	Fe I	6546.239	2.76	-1.54
Fe I	6079.009	4.65	-1.13	Fe I	6569.215	4.73	-0.42
Fe I	6082.711	2.22	-3.57	Fe I	6575.016	2.59	-2.82
Fe I	6093.644	4.61	-1.51	Fe I	6593.870	2.43	-2.42
Fe I	6096.665	3.98	-1.93	Fe I	6597.561	4.79	-1.06
Fe I	6105.131	4.55	-2.06	Fe I	6608.026	2.28	-4.04
Fe I	6151.623	2.18	-3.30	Fe I	6609.110	2.56	-2.69
Fe I	6157.733	4.07	-1.25	Fe I	6627.545	4.55	-1.68
Fe I	6173.336	2.22	-2.88	Fe I	6633.412	4.83	-1.49
Fe I	6180.204	2.73	-2.78	Fe I	6633.750	4.56	-0.78
Fe I	6187.990	3.94	-1.72	Fe I	6634.107	4.79	-1.43
Fe I	6200.313	2.61	-2.44	Fe I	6646.934	2.61	-3.99
Fe I	6213.430	2.22	-2.65	Fe I	6703.567	2.76	-3.15
Fe I	6219.280	2.20	-2.43	Fe I	6704.476	4.22	-2.66
Fe I	6220.794	3.88	-2.46	Fe I	6710.319	1.48	-4.87
Fe I	6240.646	2.22	-3.39	Fe I	6713.745	4.79	-1.60
Fe I	6254.258	2.28	-2.48	Fe I	6716.237	4.58	-1.93
Fe I	6265.134	2.18	-2.55	Fe I	6725.357	4.10	-2.30
Fe I	6270.225	2.86	-2.71	Fe I	6726.667	4.61	-1.00
Fe I	6280.618	0.86	-4.39	Fe I	6733.151	4.64	-1.57
Fe I	6297.793	2.22	-2.74	Fe I	6750.152	2.42	-2.60
Fe I	6302.494	3.69	-0.91	Fe I	6752.707	4.64	-1.37
Fe I	6311.500	2.83	-3.22	Fe I	6786.860	4.19	-2.06
Fe I	6315.811	4.07	-1.71	Fe I	6793.259	4.07	-2.47
Fe I	6322.685	2.59	-2.43	Fe I	6806.845	2.73	-3.21
Fe I	6335.331	2.20	-2.18	Fe I	6810.263	4.61	-1.11
Fe I	6336.824	3.69	-1.05	Fe I	6820.372	4.64	-1.31
Fe I	6344.149	2.43	-2.92	Fe I	6828.591	4.64	-0.92
Fe I	6355.029	2.84	-2.29	Fe I	6841.339	4.61	-0.75
Fe I	6380.743	4.19	-1.40	Fe I	6842.686	4.64	-1.31
Fe I	6419.950	4.73	-0.25	Fe I	6843.656	4.55	-0.93
Fe I	6430.849	2.18	-2.01	Fe I	6855.162	4.56	-1.82
Fe I	6475.624	2.56	-2.94	Fe I	6978.852	2.48	-2.50
Fe I	6481.970	2.28	-2.98	Fe I	7038.223	4.22	-1.31
Fe I	6495.742	4.83	-0.94	Fe I	7068.410	4.07	-1.38
Fe I	6496.467	4.79	-0.57	Fe I	7090.383	4.23	-1.21
Fe I	6498.939	0.96	-4.70	Fe I	7130.922	4.22	-0.78
Fe I	6518.367	2.83	-2.75	Fe I	7132.986	4.07	-1.75
Fe I	6533.929	4.56	-1.45	Fe I	7401.685	4.19	-1.69

TABLE 6
FE II LINE LIST.

Ion	$\lambda(\text{\AA})$	χ_{ex}	log gf	Ion	$\lambda(\text{\AA})$	χ_{ex}	log gf
Fe II	4508.29	2.85	-2.21	Fe II	5325.55	3.22	-2.60
Fe II	4515.34	2.48	-2.48	Fe II	5414.07	3.22	-3.36
Fe II	4520.22	2.81	-2.61	Fe II	5425.26	3.20	-3.79
Fe II	4534.17	2.85	-3.48	Fe II	5534.85	3.24	-2.92
Fe II	4555.89	2.83	-2.28	Fe II	6084.105	3.20	-4.06
Fe II	4576.34	2.03	-3.04	Fe II	6113.329	3.22	-4.35
Fe II	4582.83	2.84	-3.09	Fe II	6233.498	4.48	-2.84
Fe II	4620.52	2.81	-3.29	Fe II	6239.948	3.89	-3.57
Fe II	4656.98	2.89	-3.63	Fe II	6247.562	3.89	-2.68
Fe II	4670.18	2.58	-4.10	Fe II	6369.463	2.89	-1.90
Fe II	4731.45	2.89	-3.37	Fe II	6383.715	4.55	-2.44
Fe II	4833.20	2.66	-4.78	Fe II	6385.458	4.55	-2.83
Fe II	4923.93	2.89	-1.32	Fe II	6416.928	3.89	-2.74
Fe II	5000.74	2.77	-4.75	Fe II	6432.683	2.89	-3.55
Fe II	5132.67	2.81	-4.17	Fe II	6456.391	3.90	-2.43
Fe II	5197.58	3.23	-2.10	Fe II	6493.060	4.58	-3.00
Fe II	5234.62	3.22	-2.05	Fe II	6516.083	2.89	-3.65
Fe II	5284.11	2.89	-3.20	Fe II	7067.460	3.8	-3.85

TABLE 7
MEASURED EQUIVALENT WIDTHS OF FE I LINES: b1 TO b17

λ	b1	b2	b3	b4	b5	b6	b7	b8	b9	b10	b11	b12	b13	b14	b15	b16	b17
6056.005	52	87	79	89	85	55	58	54	86	103	63	95	47	77	53	52	70
6079.009	31	60	47	68	54	-	33	38	49	76	37	62	23	62	44	36	51
6082.711	27	56	52	67	51	-	29	34	51	66	-	73	15	65	28	30	33
6093.644	23	44	40	55	41	24	18	27	44	58	24	51	15	44	20	20	38
6096.665	25	53	50	64	51	25	26	32	52	68	38	73	20	62	30	25	40
6105.131	7	24	16	41	19	-	6	-	67	34	10	31	-	18	8	14	15
6151.623	39	68	67	79	65	43	42	47	59	82	45	86	29	79	37	43	49
6157.733	43	78	69	91	70	50	50	60	81	90	55	93	40	83	48	48	66
6173.336	54	87	82	100	85	51	60	-	83	99	66	110	48	98	52	57	13
6180.204	37	76	69	87	72	39	43	64	72	102	48	91	30	80	29	46	60
6187.990	28	69	56	78	63	29	-	-	-	72	40	75	24	65	33	31	49
6200.313	48	94	82	110	89	52	65	64	90	116	65	105	48	93	18	57	70
6213.430	64	113	90	111	106	63	73	75	96	118	76	115	58	102	64	60	80
6220.794	-	29	23	43	-	-	-	-	-	50	85	41	7	36	18	14	-
6232.641	-	98	99	113	107	63	71	70	100	-	75	116	51	115	72	82	50
6240.646	32	71	45	79	63	34	41	43	64	85	44	80	31	68	37	40	50
6254.258	100	136	126	153	137	-	100	-	-	157	118	156	91	143	90	10	124
6265.134	71	-	108	122	108	77	79	78	100	-	83	-	-	137	67	76	90
6270.225	49	-	63	86	65	46	42	46	69	-	49	-	-	79	41	42	60
6280.618	56	-	90	103	103	-	-	67	-	-	65	-	-	109	63	66	70
6297.793	84	106	93	111	119	73	70	72	90	110	72	123	54	113	56	63	73
6302.494	64	101	97	110	109	72	71	77	105	140	79	142	58	124	63	48	85
6311.500	16	44	44	58	44	18	21	22	52	59	25	72	13	53	25	23	28
6315.811	28	59	49	68	54	32	36	31	59	69	35	71	23	56	26	51	48
6322.685	59	96	96	115	96	67	-	75	91	116	74	121	53	114	59	65	76
6335.331	86	118	115	135	126	89	87	91	119	142	94	174	79	154	78	88	100
6336.824	83	115	123	134	144	91	-	-	165	101	192	78	174	83	82	104	-
6344.149	-	73	72	-	81	48	51	51	71	95	52	93	39	95	50	52	-
6355.029	58	99	97	128	101	55	62	66	98	129	70	122	47	118	55	45	82
6380.743	37	66	56	78	64	41	39	45	65	81	52	72	28	55	40	35	49
6419.950	60	99	90	112	102	66	71	70	99	124	77	103	57	97	-	15	89
6430.849	90	125	139	155	-	100	101	109	137	170	108	225	88	193	89	10	100
6475.624	37	71	72	90	77	43	45	50	69	98	53	100	41	84	38	48	59
6481.970	49	81	80	99	90	54	55	62	78	100	60	109	42	98	51	54	-
6495.742	25	51	47	66	48	-	29	-	51	76	-	76	23	62	27	28	43
6496.467	49	74	78	90	74	44	45	44	79	109	53	88	36	85	49	46	66
6498.939	30	60	66	85	65	39	41	-	65	83	43	99	30	90	31	59	52
6518.367	40	72	74	88	71	46	47	54	71	-	-	-	90	45	44	62	-
6533.929	20	51	50	70	-	27	23	28	49	69	33	61	20	55	25	25	46
6546.239	76	115	118	134	133	-	104	96	123	155	100	163	82	158	90	95	98
6569.215	54	83	81	96	90	52	61	60	85	107	62	102	49	94	62	55	74
6575.016	41	80	70	94	79	45	53	57	77	97	56	110	40	96	52	54	57
6593.870	67	104	95	113	109	66	76	-	103	125	103	123	82	111	64	71	81
6597.561	28	55	51	65	56	29	33	33	51	75	34	63	22	52	27	32	46
6608.026	9	30	27	44	29	-	15	13	31	49	18	53	8	42	13	18	20
6609.110	51	-	77	108	86	54	61	56	82	111	60	106	41	84	52	51	66
6627.545	17	44	37	54	37	18	18	20	38	55	23	54	15	45	15	18	27
6633.412	14	38	35	63	37	16	17	55	38	61	23	64	14	52	19	19	35
6633.750	48	79	77	93	77	51	50	32	75	98	58	94	41	86	47	51	68
6634.107	24	-	46	-	42	25	21	-	48	-	34	73	17	55	39	24	52
6646.932	-	19	20	33	16	-	-	-	-	-	-	-	-	33	6	7	-
6703.567	23	54	54	72	49	28	34	32	50	73	34	66	19	70	28	33	41
6710.319	8	28	30	53	26	-	-	-	-	51	18	66	6	50	11	14	16
6713.745	15	28	35	47	29	18	-	-	-	43	18	-	-	57	13	-	26
6716.237	10	27	25	39	27	-	-	-	-	42	16	43	7	28	16	10	20
6725.357	15	28	28	41	25	12	-	-	-	75	16	46	-	37	13	10	17
6726.667	28	59	59	69	59	38	33	38	56	75	43	76	28	68	33	33	55
6733.151	14	39	38	55	32	17	15	21	37	53	22	51	13	39	17	17	29
6750.152	56	93	86	108	89	60	64	67	89	112	70	102	52	98	60	61	73
6752.707	-	50	43	73	45	25	21	26	42	72	31	67	18	43	27	20	36
6786.860	-	40	35	49	33	15	15	17	34	50	21	43	11	36	-	15	26
6793.259	-	21	19	36	20	-	8	10	19	32	13	28	-	25	9	8	12
6806.845	20	52	47	66	46	23	28	29	50	70	34	68	16	60	24	27	35
6810.263	35	63	58	77	60	36	35	41	62	81	40	68	24	66	34	34	52
6820.372	27	57	51	68	-	32	25	31	50	71	35	7	22	58	27	28	41
6828.591	42	69	67	82	68	42	41	46	67	89	51	84	33	75	42	41	65
6841.339	53	76	83	96	85	58	53	60	-	109	64	-	40	88	53	48	-
6842.866	24	47	30	55	48	28	27	33	50	65	33	64	17	57	26	-	-
6943.656	-	70	72	91	74	44	49	55	73	88	57	86	35	80	42	55	-
6855.162	58	84	79	103	85	60	58	59	85	103	65	102	-	95	53	54	68
6978.852	64	91	84	110	98	61	67	68	92	113	76	95	51	99	77	65	82
7038.223	48	75	77	106	-	50	48	59	-	95	57	-	40	104	45	46	64
7068.410	48	84	80	118	81	38	47	57	85	76	62	113	38	100	38	30	70

TABLE 7—*Continued*

λ	b1	b2	b3	b4	b5	b6	b7	b8	b9	b10	b11	b12	b13	b14	b15	b16	b17
7090.383	51	83	81	98	81	57	51	56	84	110	62	111	39	98	45	53	69
7130.922	68	109	99	138	111	67	73	74	104	136	80	139	63	130	60	69	96
7132.986	32	53	50	65	53	32	36	33	52	69	36	-	23	56	26	30	49
7401.685	34	56	50	71	54	-	-	-	-	-	36	-	-	54	25	34	52

TABLE 8
MEASURED EQUIVALENT WIDTHS OF FE I LINES: B18 TO B35

λ	b18	b19	b20	b21	b22	b23	b24	b25	b26	b27	b28	b29	b30	b31	b32	b33	b34	b35
6056.005	66	75	42	57	63	79	59	64	61	86	73	67	47	66	57	-	-	51
6079.009	36	47	28	41	38	46	34	39	32	54	-	40	30	35	28	23	22	29
6082.711	32	45	-	30	34	36	-	48	30	51	30	25	21	34	18	20	24	-
6093.644	26	38	19	26	22	37	25	28	22	45	31	27	15	21	-	-	-	14
6096.665	35	49	26	30	32	39	30	37	26	56	37	30	22	33	22	17	23	22
6105.131	10	23	-	-	11	-	10	12	-	24	12	9	-	-	-	-	-	-
6151.623	49	64	41	37	46	49	40	62	42	68	48	44	34	51	33	31	42	33
6157.733	55	76	41	50	55	65	50	63	54	77	62	56	43	53	43	44	42	41
6173.336	63	78	52	57	64	70	56	81	62	87	64	61	52	63	46	50	51	49
6180.204	49	69	34	41	51	60	46	65	47	73	49	49	36	55	36	34	36	36
6187.990	39	54	27	36	42	48	36	49	38	59	43	41	27	40	30	29	28	28
6200.313	65	77	-	61	63	75	64	82	66	85	74	68	59	71	56	55	46	52
6213.430	76	87	59	66	75	88	71	93	78	93	81	77	69	86	66	66	56	66
6220.794	-	95	-	80	-	-	-	-	-	103	-	-	-	-	-	72	61	72
6232.641	-	-	-	-	-	-	-	-	-	66	-	-	-	-	-	30	33	33
6240.646	45	54	30	33	41	51	40	62	44	135	44	42	33	49	30	-	-	-
6254.258	117	137	80	10	118	11	-	121	-	106	-	91	-	111	76	65	72	67
6265.134	85	103	70	76	82	88	76	99	80	70	86	80	68	90	73	34	34	34
6270.225	52	66	39	36	54	54	45	62	44	92	50	45	35	50	30	44	-	47
6280.618	69	99	88	51	62	-	-	89	67	96	-	-	-	78	-	54	63	56
6297.793	68	92	62	65	72	78	67	87	69	101	-	69	70	100	60	81	-	62
6302.494	75	99	87	85	76	10	73	77	75	43	82	76	68	84	-	11	-	13
6311.500	28	44	-	22	27	30	18	39	20	57	23	22	18	34	-	22	26	21
6315.811	35	51	28	31	67	45	33	42	31	99	42	36	23	34	24	53	58	60
6322.685	72	92	59	62	78	78	67	83	72	121	75	70	58	76	59	78	78	78
6335.331	91	118	84	86	95	99	87	106	93	131	97	90	82	103	82	76	-	-
6336.824	93	136	88	92	102	10	92	101	-	-	103	95	-	109	77	-	-	-
6344.149	-	-	47	49	53	-	-	71	-	101	-	-	-	-	-	52	48	50
6355.029	69	95	54	62	71	80	67	91	69	58	72	66	56	72	50	31	-	36
6380.743	46	55	31	38	44	51	43	53	45	96	50	49	37	38	41	63	51	63
6419.950	72	86	55	67	78	87	72	74	75	136	88	78	64	74	67	93	-	93
6430.849	108	131	98	10	110	11	10	124	10	72	105	105	95	-	95	-	45	36
6475.624	52	72	35	53	49	66	44	69	49	84	54	53	36	53	41	44	52	47
6481.970	61	78	52	49	61	67	56	76	58	57	65	59	50	71	48	33	-	20
6495.742	41	45	-	37	153	38	27	34	-	81	36	32	19	-	-	43	49	44
6496.467	53	68	46	53	57	74	51	56	52	66	56	43	56	39	26	35	29	29
6498.939	45	66	42	28	43	46	36	69	41	74	41	35	31	53	25	46	43	43
6518.367	54	73	46	43	55	60	49	65	49	-	54	54	42	-	40	23	-	-
6533.929	33	46	82	32	-	40	27	34	27	121	36	31	-	18	-	79	78	83
6546.239	100	119	-	85	96	10	98	122	97	84	102	92	89	113	88	54	44	51
6569.215	61	76	48	56	68	72	61	68	63	74	73	66	51	68	55	42	45	40
6575.016	60	76	41	46	53	61	52	74	56	98	56	68	44	62	54	63	54	63
6593.870	78	88	83	68	78	84	75	95	79	54	83	79	67	88	66	23	-	21
6597.561	37	46	29	33	39	48	34	38	34	29	42	35	27	34	24	-	-	12
6608.026	18	31	11	10	18	21	13	29	13	81	12	13	-	23	-	45	43	49
6609.110	56	76	45	51	59	70	55	75	58	44	62	61	48	65	47	-	-	15
6627.545	21	35	20	22	23	32	19	26	20	40	27	22	-	21	15	-	-	16
6633.412	24	37	18	19	22	31	18	26	20	77	28	23	13	16	17	44	44	48
6633.750	58	77	51	54	59	65	54	60	56	-	62	58	45	55	47	-	-	-
6634.107	32	44	25	25	34	-	-	40	-	-	-	-	-	26	-	-	-	-
6646.932	-	15	-	-	-	-	-	15	-	55	10	8	-	-	7	22	-	22
6703.567	31	47	26	28	32	38	30	48	29	-	33	31	21	33	23	-	-	-
6710.319	15	26	-	-	14	-	12	32	12	-	11	11	-	18	-	-	-	-
6713.745	19	49	-	23	20	27	-	18	14	29	22	18	-	11	-	-	-	-
6716.237	-	19	8	-	12	18	-	18	10	29	-	11	-	-	-	-	-	-
6725.357	16	28	-	13	-	20	11	20	13	62	16	15	-	-	-	23	-	31
6726.667	40	58	33	39	44	48	35	42	37	33	46	41	31	38	-	-	-	-
6733.151	23	34	15	20	21	28	21	26	17	88	22	20	-	-	17	56	-	57
6750.152	67	81	50	60	66	73	64	85	67	48	72	67	59	72	-	16	19	19
6752.707	29	42	20	30	30	33	28	35	27	34	36	30	22	26	19	-	-	-
6786.860	16	31	13	18	24	24	14	25	16	-	19	22	-	-	-	-	-	-
6793.259	-	16	-	-	-	-	9	14	-	53	-	-	-	-	-	21	-	21
6806.845	32	44	23	26	29	38	27	47	28	61	32	26	22	33	20	33	-	30
6810.263	40	54	30	40	43	54	42	44	40	56	47	43	31	43	34	21	-	24
6820.372	27	57	51	68	-	32	25	31	50	71	35	7	22	58	27	28	41	-
6828.591	42	69	67	82	68	42	41	46	67	89	51	84	33	75	42	41	65	-
6841.339	53	76	83	96	85	58	53	60	-	109	64	-	40	88	53	48	-	-
6842.866	24	47	30	55	48	28	27	33	50	65	33	64	17	57	26	-	-	-
6943.656	-	70	72	91	74	44	49	55	73	88	57	86	35	80	42	55	-	-
6855.162	58	84	79	103	85	60	58	59	85	103	65	102	-	95	53	54	68	-
6978.852	64	91	84	110	98	61	67	68	92	113	76	95	51	99	77	65	82	-
7038.223	48	75	77	106	-	50	48	59	-	95	57	-	40	104	45	46	64	-
7068.410	48	84	80	118	81	38	47	57	85	76	62	113	38	100	38	30	70	-

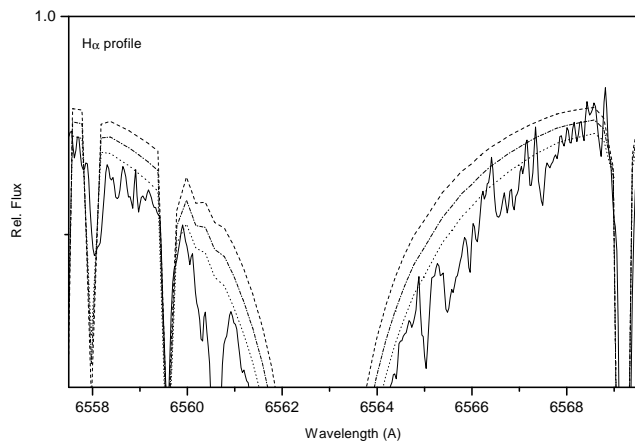


Fig. 1.— Observed $H\alpha$ profile (solid line) of HD 179764, and synthetic spectra for $T_{\text{eff}} = 5550$ K (dotted line), $T_{\text{eff}} = 5350$ K (dashed line), and the best fit for $T_{\text{eff}} = 5450$ K (dash-dotted line)

TABLE 8—*Continued*

λ	b18	b19	b20	b21	b22	b23	b24	b25	b26	b27	b28	b29	b30	b31	b32	b33	b34	b35
7090.383	51	83	81	98	81	57	51	56	84	110	62	111	39	98	45	53	69	
7130.922	68	109	99	138	111	67	73	74	104	136	80	139	63	130	60	69	96	
7132.986	32	53	50	65	53	32	36	33	52	69	36	-	23	56	26	30	49	
7401.685	34	56	50	71	54	-	-	-	-	-	36	-	-	54	25	34	52	

TABLE 9
MEASURED EQUIVALENT WIDTHS OF Fe II LINES: B1 TO B17

λ	b1	b2	b3	b4	b5	b6	b7	b8	b9	b10	b11	b12	b13	b14	b15	b16	b17
4508.29	80	104	77	100	81	78	65	79	84	85	79	65	68	61	71	46	100
4515.34	73	102	83	108	87	70	58	78	84	115	78	95	59	-	69	51	96
4520.22	75	93	74	95	79	73	62	77	77	85	76	72	58	67	68	49	91
4534.17	48	62	44	63	45	42	28	41	46	56	44	-	28	32	-	17	62
4555.89	83	103	82	107	89	77	65	83	86	87	81	63	66	-	68	58	-
4576.34	-	-	53	-	56	-	-	57	-	64	54	-	41	39	49	-	71
4582.83	46	-	-	90	53	41	37	47	61	-	45	-	31	-	38	-	64
4620.52	45	76	49	75	47	46	35	53	55	73	48	-	31	32	42	-	60
4656.98	27	48	91	46	24	-	-	27	30	34	22	-	-	-	23	11	40
4670.18	22	48	29	48	28	19	12	24	37	34	24	-	12	17	-	-	38
4731.45	-	-	78	-	81	-	-	-	-	91	71	-	-	-	-	-	-
4833.20	9	-	10	24	-	-	-	11	12	-	8	-	-	-	-	-	17
4923.93	134	181	135	171	153	133	111	136	140	148	137	100	11	101	123	99	171
5000.74	-	-	7	15	5	-	-	7	-	8	3	-	-	-	-	-	11
5132.67	-	-	-	-	15	21	-	22	27	-	17	-	-	-	16	-	32
5197.58	71	-	72	97	75	66	60	74	79	90	-	46	57	42	67	34	89
5234.62	76	99	72	95	77	78	58	81	77	80	-	51	61	47	61	-	84
5284.11	52	-	62	81	64	51	41	57	65	70	55	-	36	-	-	29	71
5325.55	-	-	32	-	33	-	-	-	-	39	31	-	-	-	-	-	-
5414.07	24	44	19	42	20	-	-	-	24	29	21	-	-	-	15	8	40
5425.26	-	-	36	-	37	-	-	-	-	42	35	-	-	-	-	-	-
5534.85	53	-	47	63	47	54	35	57	53	55	49	35	36	31	-	-	72
6084.10	-	32	17	35	17	18	10	18	19	28	-	14	14	-	-	-	-
6113.33	6	28	8	22	11	-	-	13	-	18	-	11	-	-	-	-	23
6196.68	-	-	-	-	-	-	-	-	-	51	-	-	-	4	-	-	-
6233.50	-	-	12	-	-	-	-	-	-	11	-	-	-	-	-	-	-
6239.95	-	26	-	-	16	-	4	-	-	-	11	-	-	-	-	-	-
6247.56	43	71	43	-	-	45	32	46	45	48	48	22	32	19	-	26	66
6369.46	13	28	13	30	-	-	-	-	18	26	17	-	8	5	-	6	-
6383.71	6	17	-	19	11	-	-	-	9	19	-	-	-	10	-	-	18
6385.46	-	15	-	-	-	-	-	-	16	-	-	-	-	-	-	-	-
6416.93	-	-	-	-	-	-	-	31	40	50	35	10	19	32	-	26	-
6432.68	38	51	36	56	33	37	23	-	37	33	37	39	22	20	-	15	59
6456.39	55	77	49	74	56	57	39	58	56	61	64	36	41	32	-	24	83
6493.06	5	-	-	-	-	-	-	-	-	-	-	-	-	-	-	-	7
6516.08	46	85	38	81	45	45	31	50	52	61	50	29	29	27	-	24	77
7067.46	7	17	-	-	15	-	-	-	11	31	-	22	5	15	-	-	14

TABLE 10
MEASURED EQUIVALENT WIDTHS OF FE II LINES: b18 TO b35

λ	b18	b19	b20	b21	b22	b23	b24	b25	b26	b27	b28	b29	b30	b31	b32	b33	b34	b35
4508.29	84	77	65	-	81	86	79	73	73	83	99	88	65	69	88	77	63	67
4515.34	71	79	56	-	75	88	68	75	63	80	97	85	59	59	83	73	-	62
4520.22	73	74	-	-	76	84	71	71	65	79	92	83	61	60	80	70	57	69
4534.17	43	42	-	-	39	53	41	38	36	46	61	50	-	-	50	37	-	36
4555.89	81	77	58	-	80	92	77	75	70	88	99	90	62	66	85	75	64	71
4576.34	-	-	-	-	-	-	-	-	49	-	75	65	-	-	-	-	-	48
4582.83	49	45	27	-	43	64	44	52	39	-	68	58	32	34	52	41	28	44
4620.52	50	44	29	-	51	56	44	42	38	51	64	45	30	35	50	40	30	38
4656.98	30	20	-	-	21	36	25	24	18	28	44	34	14	15	32	20	15	20
4670.18	24	25	11	-	22	32	18	22	16	26	36	30	11	16	25	17	17	18
4731.45	-	-	-	-	-	-	-	-	64	-	-	-	-	-	-	-	-	59
4833.20	-	-	-	-	7	12	9	-	-	-	-	-	-	-	9	-	-	-
4923.93	137	132	101	-	137	150	130	119	12	141	164	-	106	117	149	127	118	12
5000.74	-	-	-	-	-	-	-	-	-	-	-	-	-	-	11	-	-	-
5132.67	20	18	9	-	19	28	17	-	-	-	29	-	-	-	22	-	-	10
5197.58	72	64	39	-	72	86	71	71	64	72	99	88	65	59	84	69	50	65
5234.62	78	58	57	-	72	88	-	67	65	78	95	86	53	63	86	69	-	66
5284.11	-	47	41	-	55	69	54	52	46	-	77	-	-	40	62	46	-	45
5325.55	-	-	-	-	-	-	-	-	22	-	-	-	-	-	-	-	-	23
5414.07	-	-	-	-	-	-	-	-	12	-	-	29	-	-	-	25	-	14
5425.26	36	-	-	-	-	-	-	-	25	-	-	-	-	-	-	-	-	27
5534.85	52	48	340	-	48	59	45	44	42	50	70	61	-	36	58	-	38	41
6084.10	22	20	-	28	20	-	-	14	11	18	34	22	-	-	24	14	-	-
6113.33	13	9	7	10	-	-	-	10	-	-	21	18	-	-	-	-	-	7
6196.68	-	-	-	-	-	-	-	-	-	-	-	-	-	-	-	-	-	-
6233.50	-	-	-	-	-	-	-	-	-	-	-	-	-	-	-	-	-	-
6239.95	-	-	-	13	9	-	-	-	-	-	23	15	-	-	13	-	-	-
6247.56	45	38	25	57	43	-	-	35	32	42	69	59	29	33	58	40	24	37
6369.46	14	-	-	20	16	-	-	11	11	19	27	20	-	8	16	14	-	-
6383.71	10	7	-	10	-	-	-	5	-	-	14	10	-	-	-	5	-	-
6385.46	-	4	-	7	-	-	-	-	-	19	-	-	-	-	-	-	-	7
6416.93	33	-	-	-	-	-	-	-	-	-	-	-	-	-	-	-	14	-
6432.68	36	26	-	46	39	-	-	31	28	38	57	-	20	19	-	27	-	31
6456.39	55	53	29	65	61	-	-	48	42	57	74	64	35	47	66	-	35	45
6493.06	-	-	-	-	-	-	-	17	-	-	-	-	-	-	-	5	-	-
6516.08	52	50	31	62	53	-	-	43	37	54	66	57	25	36	56	42	32	42
7067.46	13	17	42	-	-	-	-	7	-	-	-	-	-	-	-	-	-	-

TABLE 11
PHYSICAL PARAMETERS

Reference	$\log g^{\text{Hip}}$	$\sigma(\log g^{\text{Hip}})$	$\log g^{\text{Spec}}$	$[\text{Fe}/\text{H}]^{\text{Gen}}$	$[\text{Fe}/\text{H}]^{\text{Spec}}$	$\xi(\text{kms}^{-1})$
b1	4.06	0.06	3.8	-0.47	-0.50	1.0
b2	3.80	0.05	3.7	0.01	0.10	0.9
b3	4.38	0.06	4.3	0.11	0.00	0.5
b4	3.68	0.07	3.6	0.27	0.26	1.1
b5	4.40	0.05	3.9	-0.08	-0.12	0.9
b6	3.76	0.20	3.7	-0.31	-0.50	0.6
b7	4.42	0.09	4.7	-0.28	-0.48	0.5
b8	3.86	0.06	4.0	-0.48	-0.33	0.6
b9	4.21	0.06	4.2	0.16	0.05	0.5
b10	4.20	0.06	4.1	0.30	0.38	0.8
b11	4.02	0.07	4.0	-0.16	-0.25	0.8
b12	4.35	0.10	3.8	0.60	0.05	1.0
b13	4.26	0.07	4.3	-0.54	-0.65	0.5
b14	4.10	0.11	4.3	0.50	-0.05	0.5
b15	4.00	0.07	4.0	-0.40	-0.55	0.5
b16	4.43	0.07	4.7	-0.27	-0.70	0.5
b17	4.13	0.07	3.7	0.09	-0.05	1.0
b18	3.76	0.07	3.8	-0.37	-0.33	0.6
b19	4.29	0.09	4.1	0.07	-0.10	0.5
b20	4.30	0.08	4.4	-0.45	-0.70	0.5
b21	4.10	0.07	3.9	-0.17	-0.22	1.0
b22	4.10	0.08	4.0	-0.18	-0.30	0.7
b23	4.10	0.06	4.1	0.00	-0.02	1.0
b24	4.26	0.05	4.0	-0.34	-0.40	0.7
b25	3.36	0.05	3.1	-0.33	-0.53	0.8
b26	4.33	0.06	4.1	-0.27	-0.50	0.9
b27	4.30	0.06	4.0	0.12	0.00	0.8
b28	3.95	0.05	3.6	0.11	-0.12	1.2
b29	4.11	0.06	4.2	-0.11	-0.25	1.0
b30	4.04	0.06	4.3	-0.46	-0.60	0.6
b31	4.30	0.07	4.0	-0.47	-0.70	0.6
b32	3.87	0.07	3.7	-0.37	-0.40	1.0
b33	4.21	0.06	4.0	-0.42	-0.60	1.0
b34	3.77	0.06	3.9	-0.19	-0.75	0.8
b35	4.31	0.08	4.1	-0.47	-0.55	0.5

TABLE 12
OXYGEN ABUNDANCES

Name	[O/Fe]	Name	[O/Fe]
HD 143016	+0.23	HD 214059	-
HD 143102	0.00	CD-40 1503	-
HD 148530	+0.33	HD 219180	-
HD 149256	+0.08	HD 220536	0.00
HD 152391	0.00	HD 220993	+0.23
HDE 326583	+0.23	HD 224383	+0.18
HD 175617	-	HD 4308	+0.18
HD 178737	+0.28	HD 6734	+0.28
HD 179764	+0.13	HD 8638	+0.23
HD 181234	-0.07	HD 9424	0.00
HD 184846	+0.23	HD 10576	0.00
BD-17 6035	0.00	HD 10785	-
HD 198245	-	HD 11306	+0.33
HD 201237	+0.08	HD 11397	+0.23
HD 211276	-	HD 14282	-
HD 211532	+0.43	HD 16623	+0.33
HD 211706	-	BD-02 603	-
HD 21543	+0.33		

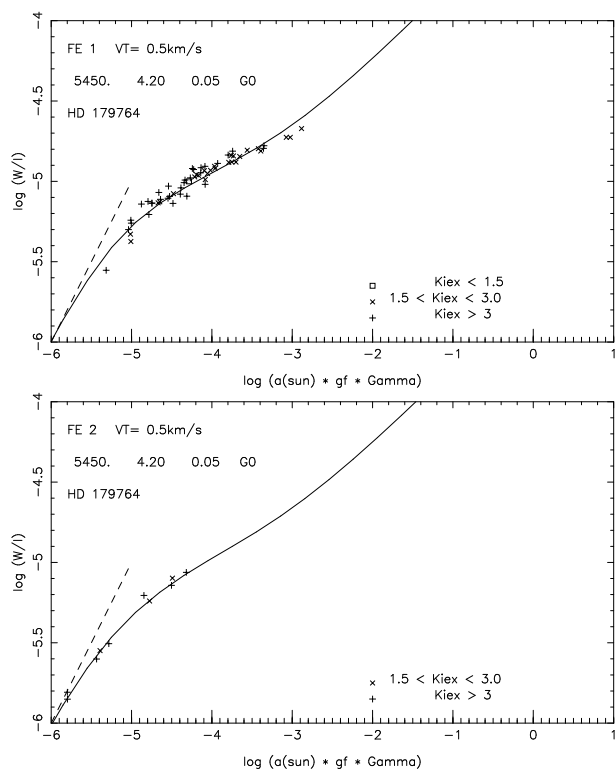


Fig. 2.— Curves of growth for Fe I and Fe II lines of HD 179764 (symbols represent the lower potentials of the lines).

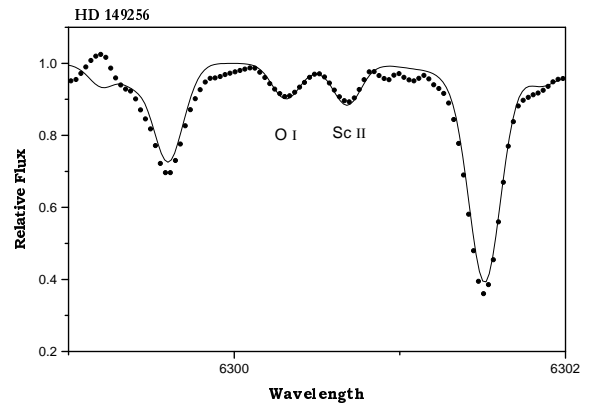
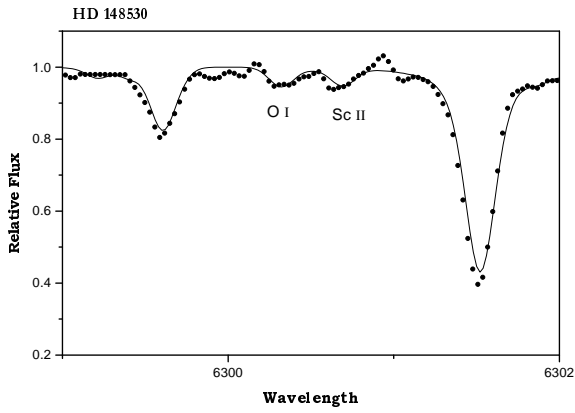


Fig. 3.— Spectrum synthesis of the [OI] line: observed (dots) and synthetic (solid lines) for HD 148530 and HD 149256.

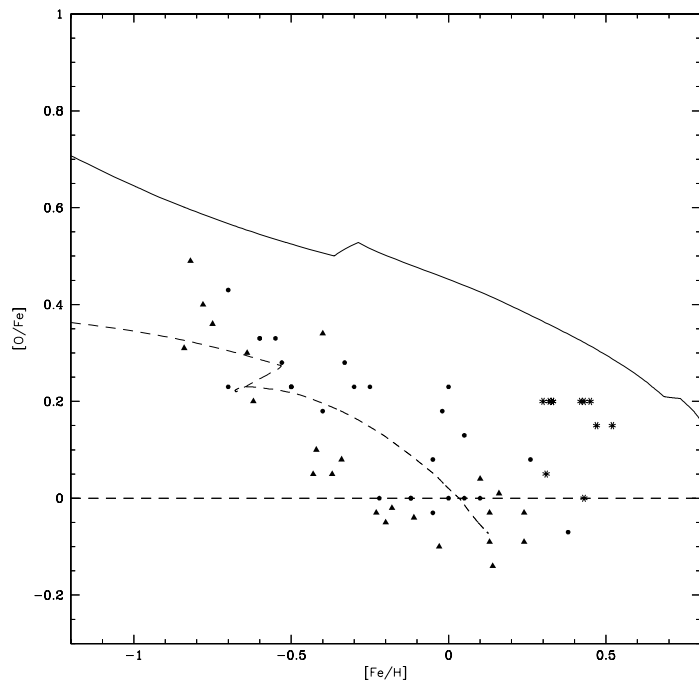


Fig. 4.— Oxygen to iron ratio for three samples: our data (circles), SMR stars of Barbuy & Grenon (1990) (stars) and a sample of disk stars (triangles) from Nissen & Edvardsson (1992). The lines are theoretical curves for bulge (solid line) and solar vicinity (dashed line), from Matteucci et al. (1999) and Chiappini et al. (2001), respectively.